Vanessa Michels
vanessa@labtucal.ufsc.br
Federal University of Santa Catarina
Mechanical Engineering Department
88040-900 Florianópolis, SC, Brazil

Fernando H. Milanez
fernando.milanez@ararangua.ufsc.br
Federal University of Santa Catarina
Energy Engineering Department
88900-000 Araranguá, SC, Brazil

Marcia B. H. Mantelli
marcia@emc.ufsc.br
Federal University of Santa Catarina
Mechanical Engineering Department
88040-900 Florianópolis, SC, Brazil

Vapor Chamber Heat Sink with Hollow Fins

A new vapor chamber heat sink with maximum fin efficiency is presented. The fins are hollow, so the vapor generated at the base flows up to the top of the fins. As a result, the heat sink is practically isothermal. A prototype of the hollow fin vapor chamber heat sink was built and tested. The prototype presented 20% less overall thermal resistance than conventional pin fin heat sinks with the same mass and volume. A theoretical model for the heat sink thermal resistance was developed and the agreement between the model and the experimental data is fair.
Keywords: *vapor chamber, heat sink, hollow fins*

Nomenclature

A	= area, m^2
d_{fin}	= fin diameter, m
h	= convection heat transfer coefficient, W/(m²K)
q	= sink heat transfer rate, W
R	= thermal resistance, K/W
t	= plate thickness, m
T	= temperature, °C

Subscripts

a	= relative to air
amb	= relative to ambient
b	= relative to boiling
$b1$	= relative to boiling on the source area
$b2$	= relative to boiling outside the source area
$cond$	= relative to condensation
$conv$	= relative to convection
m	= relative to material
s	= relative to spreading
v	= relative to vapor
w	= relative to tube wall

Introduction

The ever-increasing heat flux levels produced by electronic devices have led to the search for more efficient and smaller heat sinks. The performance of traditional air-cooled heat sink approach, i.e., a solid base plate with attached fins, requires thermal gradients to appear. That is because they are based on thermal conduction of solids. On the other hand, the vapor chamber heat sink approach is based on phase-change heat transfer, which requires smaller thermal gradients. The smaller the thermal gradients inside the heat sink, the smaller the overall thermal resistance of the heat sink.

There are innumerous woks in the literature dealing with the modeling and optimization of traditional heat sinks, like Culham et al. (2001), Khan et al. (2003), Muzychka (2003). The typical geometry of a conventional heat sink is shown in Fig. 1. The base plate spreads the heat from the electronic device to a larger area, where the fins are attached. The heat is then eliminated to the ambient air through the fins. The back surface of the base plate, which is not in contact with the fins, can be generally considered adiabatic. The heat sink overall thermal resistance is defined as:

$$R_{overall} = \frac{T_{source} - T_{amb}}{q} \tag{1}$$

where T_{source} and T_{amb} are the heat source and the ambient temperatures, respectively, and q is the heat transfer rate through the sink. It can be divided in three parts:

$$R_{overall} = R_s + R_m + R_{fins} \tag{2}$$

Muzychka et al. (2003) presents the analytical solution developed by Yovanovich and co-workers for the spreading resistance R_s of the base-plate. The base material resistance R_m corresponds to one-dimensional heat conduction through a slab of finite thickness and area and is well known from classical heat transfer books (Incropera and De Witt, 1992). The thermal resistance of the fins R_{fins} is also known from the classical heat transfer literature. This resistance takes into account both the conduction inside the fin and the film resistance, i.e., the resistance associated to the convection heat transfer between the fins surface and the air. According to Culham et al. (2001), who studied the influence of material properties and spreading resistance in the thermal design of plate fin heat sinks, the film resistance can be as high as 80-90% of the overall thermal resistance of the heat sink. Khan et al. (2003) studied the role of fin geometry in heat sink performance. They employed an entropy generation method to show that the circular shape is the most suitable for fins, especially at relatively low air velocities.

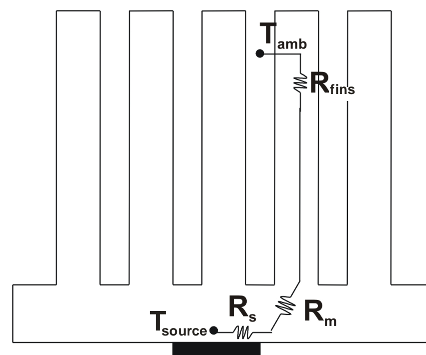

Figure 1. Conventional heat sink approach.

Paper received 9 August 2010. Paper accepted 28 February 2012
Technical Editor: Horácio Vielmo

Another heat sink approach, the vapor chamber approach, has been developed in the last two decades (Koito et al., 2003; Mochizuki, 2006 and 2008). The main difference between the vapor chamber heat sink and the conventional one is inside the base plate, which is hollow in the vapor chamber concept. Inside the vapor chamber there is a small amount of saturated working fluid. Heat coming from the heat source vaporizes the liquid, and the vapor spreads evenly on the entire chamber surface internal walls, where it condenses and returns by gravity to the evaporation section. Therefore, the vapor flow acts as heat spreader, replacing the conduction of the conventional heat sink base plate. The advantage of using vapor chamber as heat spreader is that the temperature gradients in the base plate are smaller than in the solid base plate concept, which in turn translates into a smaller spreading resistance R_s in Eq. (2). Mochizuki et al. (2008) presents a review of the designs employed over the last years for personal computer cooling. The vapor chamber concept presents the lowest overall thermal resistance among all the concepts implemented so far. Koito et al. (2003) verified that the use of a vapor chamber leads to a more uniform temperature distribution in the heat sink.

The main disadvantage of the vapor chamber heat spreader is the gravitational orientation. The heat source must be located at the lower part of the chamber, where the liquid accumulates. In order to minimize this problem, porous media, such as fine mesh screens or sintered metal powder layers have been applied to wet the evaporation section. Mochizuki et al. (2006) tested both porous media and concluded that a combination of sintered copper powder over the heat source with 200 mesh screen over the remaining area yielded the best result. The metal screen offers less friction for the return of the condensate to the evaporation area while the sintered powder over the evaporation area itself helps keeping it wet for larger heat fluxes. Despite not eliminating the problem completely, the use of porous media allows the vapor chamber to operate in non-horizontal orientations.

Vapor Chamber with Hollow Fins

The conception being proposed here is to use hollow fins instead of conventional solid fins. The fin void communicates with the vapor chamber of the base plate. Figure 2 shows a schematic of the concept. The working fluid vaporized at the base can reach the top of the fins. As a result, the fins are virtually isothermal. The fins operate in a manner similar to the condensers of two-phase thermosyphons. In fact, the hollow fin heat sink is a type of two-phase thermosyphon, which is in turn a type of heat pipe. In the classical heat pipe, the condensate returns to the evaporator zone through capillary forces of a porous structure, like small sintered metal particles or metal mesh layers. In the two-phase thermosyphon, the liquid returns by means of gravity only. In the hollow fin heat sink, the fluid condensation film moves by gravity toward the main base chamber and then, like a regular vapor chamber, it spreads over the heating area by means of a porous structure.

Two-phase thermosyphons and heat pipes have been developed by the authors in the last decades for a large variety applications, like heat exchangers (Molz et al., 2004), cooking ovens (Milanez and Mantelli, 2006a) and industrial heaters (Milanez and Mantelli, 2006b; Angelo et al., 2007). The main advantage of two-phase heat transfer devices, like the hollow fin vapor chamber heat sink, is the surface temperature uniformity. Recalling the definition of fin efficiency (Incropera and De Will, 1992), i.e., the heat transfer rate of the actual fin divided the heat transfer rate of an isothermal fin at the fin base temperature, one concludes that the hollow fin has virtually 100% efficiency. That means the fins resistance R_{fins} is negligible and consequently the heat sink overall resistance (Eq. (2)) becomes smaller.

The main objective of this work is to demonstrate that the hollow fin vapor chamber approach leads to a smaller overall heat sink thermal resistance than the conventional heat sink approach. A prototype was built and tested. Also, a theoretical model for the thermal resistance of the hollow fin vapor chamber heat sink is developed and compared with the obtained data. The results are also compared against theoretical predictions from the literature for the conventional heat sink approach.

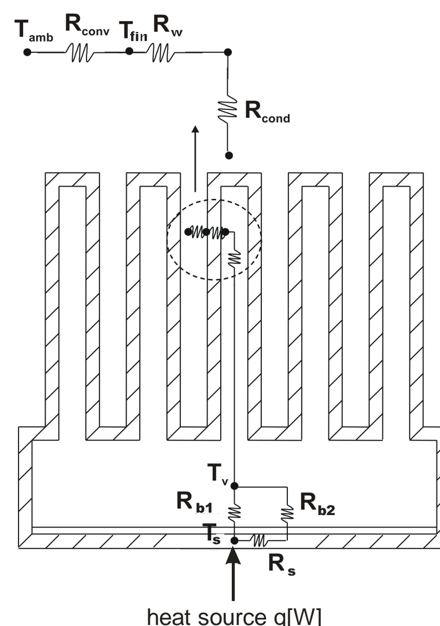

Figure 2. Vapor chamber heat sink hollow fin concept.

Experimental Study

Figure 3 shows pictures of the main parts of the prototype of the hollow fin vapor chamber heat sink. It was made of thin copper plates and tubes. The tubes (hollow fins) are soldered to the top chamber plate (Fig. 3.b) in a staggered arrangement. Six 160-mesh size brass screens were spot-welded on the lower chamber plate (Fig. 3.a) as porous media. After appropriate cleaning, the upper and lower chamber plates were bolted together through a flange. A rubber gasket between the upper and lower plates provided appropriate sealing. After assembly, the flange was thermally insulated so it did not participate in the heat transfer. The heat sink base dimensions are 130 x 135 x 9 mm, excluding the flange. The 77 fins were made of 9.53 mm external diameter copper tubes with 0.39 mm wall thickness and are 63 mm high.

The chamber was evacuated and charged with the working fluid (distilled water) through a small copper tube inserted and soldered on the chamber lateral wall (Fig. 3.a). The back side of the lower plate was also insulated. It is convenient to mention that the manufacturing procedure employed here is suitable only for laboratory tests. For industrial scale production, a more appropriate procedure should be developed.

During the tests, the prototype was air cooled by a 2.88 W electronics fan placed on the top of the fins. The heat sink temperature distribution was measured through 38 K-type thermocouples. The heat source was a 45 x 45 mm copper block with cartridge heaters inserted. The power input tested ranged from 25 to 250 W. Five working fluids filling ratios were tested, ranging

from 15 to 60% of the base chamber volume. Even for the smallest filling ratio tested, there was more than enough liquid to saturate the 6 screens layers welded to the chamber base.

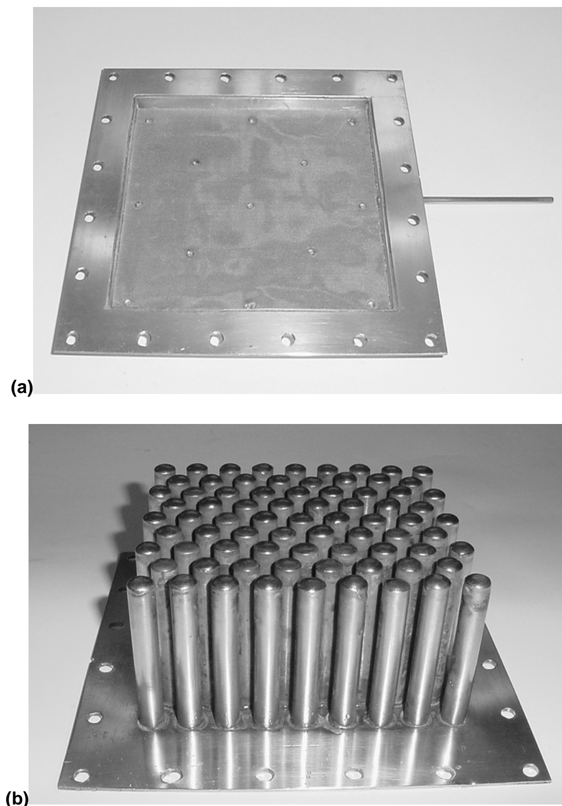

Figure 3. Prototype parts.

For every power input tested, the heat sink overall thermal resistance $R_{overall}$ was computed through Eq. (1). Also, the heat sink thermal resistance R_{sink} was computed as:

$$R_{sink} = \frac{(T_{source} - T_{fin})}{q} \tag{3}$$

where T_{fin} is the fin external surface temperature.

The sink resistance defined above does not take into account the film resistance, i.e., it is related to the heat transfer occurring inside the heat sink. The fins temperature T_{fin} was calculated as the average of the readings of 22 thermocouples spread over the fins external surface. During the tests, approximately 95% of the thermocouple readings spread within a 2°C range. As the uncertainty of the thermocouple temperature measurements are ±0.8°C, one concludes that the fins are practically isothermal. The uncertainty of thermal resistance measurements range between 5 and 10%, depending on the heat power dissipated.

Theoretical Analysis

The total thermal resistance of the hollow fin vapor chamber heat sink is analyzed using the equivalent thermal resistance network model shown in Fig. 2. The R_{b1} thermal resistance is related to the boiling heat transfer taking place right above the heat source, while R_{b2} is related to the boiling taking place outside the heat source area, and R_s is the spreading resistance of the chamber wall. As the chamber wall is relatively thin and large (1.65 x 130 mm), R_s is large and has little impact on the total thermal resistance of the network. Therefore, it is assumed that the only heat transfer from the heat source is by boiling, taking place right above the heat source area. The thermal resistance across the chamber thin copper wall is also neglected. The same is valid for R_w, the fins wall conduction resistance shown in Fig. 2. Therefore, the overall and the heat sink thermal resistance are reduced, respectively, to:

$$R_{overall} = R_{b1} + R_{cond} + R_{conv} \tag{4}$$

$$R_{sink} = R_{b1} + R_{cond} \tag{5}$$

The condensation thermal resistance and the boiling thermal resistance are obtained, respectively, from:

$$R_{cond} = \frac{1}{A_{cond} h_{cond}} \tag{6}$$

$$R_{b1} = \frac{1}{A_{source}\, h_b} \tag{7}$$

The boiling heat transfer coefficient h_b is obtained from literature correlations. Carey (1995) presents several correlations obtained from experimental data for the heat transfer coefficient in pool boiling. The presence of the wick on the vapor chamber base creates difficulties for the vapor bubbles to depart from the hot vapor chamber wall. Therefore, correlations based on pool boiling are perhaps not ideal, but are employed here anyway given the lack of specific correlations for the case under study.

The condensation heat transfer coefficient h_{cond} is also obtained from literature correlations. As the condenser of the heat sink is composed of several hollow fins that are identical to the condenser of a two-phase thermosyphon, the correlations from Kaminaga et al. (1997) and Groll and Rosler (1992), which were developed for two-phase thermosyphons, were employed here. However, a preliminary sensibility study developed by the authors showed that the condensation resistance R_{cond} in Eq. (5) represents only 3% of the sink resistance R_{sink} and is neglected here. This is due to the condensation area being much larger than the boiling area and also the condensation heat transfer coefficient being larger than the boiling coefficient. Therefore, $R_{cond} = 0$, and the boiling resistance controls the heat sink thermal resistance, i.e.:

$$R_{sink} = R_{b1} = \frac{1}{A_{source}\, h_b} \tag{8}$$

Results

Figure 4 presents both the measured and the predicted values of the heat sink thermal resistance as a function of the power output of the heat source. As already mentioned, the prototype was tested with five different levels of filling ratio. As one can see, the filling ratio affects the heat sink thermal resistance, calculated from Eq. (3). The largest thermal resistance values were obtained for the filling ratios of 15% and 20%. The results suggest that there is no working fluid enough in these tests, at least over the heat source. The other filling ratio data sets (25%, 35% and 60%) present considerably lower thermal resistances. For these three filling ratio data sets, the thermal resistance initially decreases with the heat source output, which is due to the increase of the internal heat transfer coefficients, specially boiling. The larger the heat source power, the more intense is the vapor mass flow and hence the convection in the liquid pool. Above 150 W, however, the thermal resistance starts increasing with

the heat transfer rate, which is an indication of dry-out. Under these conditions, the wick is not able to drive the condensate back over the heat source efficiently. The 25% filling ratio was the best for the prototype tested because it yielded the lowest thermal resistance, which is in the range of 0.12°C/W to 0.20°C/W. The smallest measured value of the thermal resistance, 0.12°C/W, was obtained under 150 W of heat transfer rate.

The theoretical prediction given by Eq. (8) is also presented in the same graph. Four different correlations, available in Carey (1995), for the boiling heat transfer coefficient h_b were used. As one can see, there are considerable differences among the theoretical values of the heat sink thermal resistance when different correlations for the boiling heat transfer coefficient are used in Eq. (8), especially for low heat transfer rate. The correlation of Forster and Zuber, presented by Carey (1995) yielded the best comparison with the 25% filling ratio data set, especially for heat transfer rates below 100 W. Above this value, the occurrence of dry-out makes the data trend to depart from the model. Therefore, at the optimum filling ratio, which is 25% for the prototype tested, the model with the correlation of Forster and Zuber for the boiling heat transfer coefficient predicts the thermal resistance fairly well until the occurrence of dry-out, which for the prototype tested occurred at approximately 100 W.

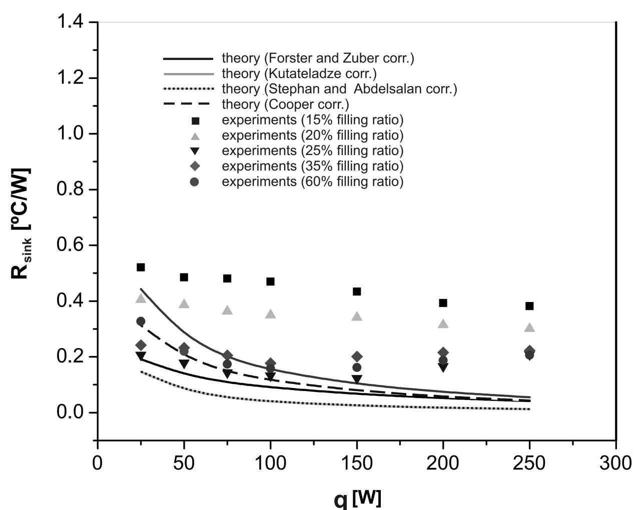

Figure 4. Heat sink thermal resistance as a function of the heat transfer rate.

Comparison with Conventional Heat Sinks

A theoretical analysis was developed in order to assess the advantages of the vapor chamber heat sink over the conventional approach. The objective is to compare the thermal resistances of the experimental prototype and of a conventional heat sink. In order to obtain a proper comparison, the conventional heat sink has the same external dimensions (135 x 130 x 72 mm) and the same mass as the prototype tested. Also, the fins of the hypothetic conventional heat sink has the same fin external geometry, i.e., cylindrical. However, the fin diameter and the base thickness of the conventional heat sink must be smaller than the hollow fin vapor chamber prototype in order to keep the mass of the two systems equal. While the prototype weights 1.01 kg, a conventional heat sink made of copper with exactly the same base thickness and fin diameter as the experimental prototype would weight approximately 4.5 kg.

Table 1 presents the thermal resistances of several conventional heat sinks with the same mass and external dimensions as the hollow fin vapor chamber prototype tested. Several configurations with different base plate thicknesses t and fin diameter d_{fin} are shown. The spreading resistance R_s was computed with the analytical model presented by Muzychka et al. (2003). The fins resistance R_{fins}, the fin efficiency η_{fin} and the material resistance R_m of the base plate were computed from analytical models available in Incropera and de Witt (1992). In this analysis, the convection heat transfer coefficient is h_{conv} = 50 W/m^{2}ºC. This value is the average of the values encountered in the experiments. The lowest overall thermal resistance of the conventional heat sink is approximately 0.38°C/W. For the best filling ratio tested, i.e. 25%, the experimental data range between 0.26°C/W and 0.34°C/W. Therefore, the overall thermal resistance of the prototype is in average 20% smaller than the resistance of the best conventional heat sink with the same weight and occupying the same volume.

Table 1. Conventional heat sink with 1.01 kg and same volume as prototype.

t [mm]	d_{fin} [mm]	R_s [ºC/W]	R_m [ºC/W]	R_{fins} [ºC/W]	$R_{overall}$ [ºC/W]	η_{fin}
1.0	4.73	0.2447	0.000142	0.232	**0.477**	0.85
1.5	4.52	0.1740	0.000214	0.242	**0.416**	0.85
2.0	4.30	0.1354	0.000285	0.254	**0.390**	0.84
3.0	3.82	0.0942	0.000427	0.285	**0.379**	0.83
4.0	3.24	0.0728	0.000570	0.329	**0.403**	0.81
5.0	2.52	0.0597	0.000712	0.406	**0.467**	0.78
6.0	1.43	0.0511	0.000855	0.604	**0.656**	0.68

If one subtracts the external convection thermal resistance, defined as $(h_{conv}.A_{film})$-1, where A_{film} is the total external surface area of the fins and the base plate, one gets an approximation for the resistance associated to conduction heat transfer in both the base plate (spreading) and the fins (fin equation). This resistance, related to the thermal gradients of conduction heat transfer, is 0.13°C/W for the best conventional heat sink. This resistance can be compared to the sink thermal resistance values presented previously in Fig. 4. As shown in this graph, the measured sink thermal resistance ranges from 0.12°C/W to 0.20°C/W for the best filling ratio. It means that the thermal resistance of the hollow fin vapor chamber heat sink is in average 20% larger than the best conventional heat sink. However, at the optimum heat transfer rate, the resistance of the vapor chamber is still 8% smaller than the pure conduction counterpart. These results show that the dominant resistance in the vapor chamber concept, the boiling resistance, is too large. As mentioned previously, the boiling resistance responds to 97% of the sink resistance. It is believed that the porous media employed, i.e. 150 mesh copper wire screens, is blocking the vapor bubbles on the evaporation surface. As already mentioned, the literature shows that layers of sintered copper powder are the most adequate porous media for vapor chambers. However, it was not available in the present study.

The 20% less overall thermal resistance of the vapor chamber heat sink with respect to the conventional approach shows the importance of the film resistance outside the heat sink. As the fins are hollow, the external heat transfer area is much larger. According to Culham et al. (2001), the film resistance is the largest part of the overall thermal resistance of a conventional heat sink. Actually, in the present experimental work, it represents approximately 70% of the heat sink overall thermal resistance. Therefore, the larger fin external surface area of the hollow fin concept leads to a decrease in the overall thermal resistance when compared to the conventional approach.

Table 2 presents the thermal resistances of the conventional heat sink with the same fin diameter and base plate thickness as the prototype tested, which weights approximately 4.5 kg. As one can see, the overall thermal resistance is below 0.17°C/W, which means the sink resistance is 0.08°C/W. This conventional heat sink has

better thermal performance than the prototype tested; however, it weighs 4.5 times more than the hollow fin vapor chamber prototype. The excess weight could pose both economical and dynamic problems.

It should be mentioned that the prototype mass could be further reduced by selecting a smaller wall thickness. During the prototype manufacturing, the wall thickness used was the smallest available commercially from stock pipes. In general, a more detailed manufacturing process development should be undertaken prior to industrial application of the concept.

Table 2. Conventional heat sink with 4.48 kg and same volume as prototype.

t [mm]	d_{fin} [mm]	R_s [°C/W]	R_m [°C/W]	R_{fins} [°C/W]	$R_{overall}$ [°C/W]	η_{fin}
9	9.53	0.0353	0.00128	0.131	**0.168**	0.93

It should be also mentioned that the comparisons with conventional heat sinks presented here are either based on same volume and mass, or on same volume and geometry as the prototype. However, there is no guarantee that the selected geometry is the optimum. For example, lower thermal resistances can be found for smaller heat sinks in detriment of increase in drag due to fluid flow around the fins. This could be true for both the conventional and the hollow fin vapor chamber heat sinks. A study similar to the one conducted by Khan et al. (2003), based on the minimization of entropy generation rate could be employed here. Also, further studies are necessary to better understand the boiling heat transfer inside the vapor chamber.

Summary and Conclusions

A new heat sink concept based on two-phase heat transfer inside a hollow fin vapor chamber was presented and analyzed here. A prototype was built and tested. The results showed that the measured sink thermal resistance depends on the working fluid filling ratio. For the prototype tested, 25% of the base chamber proved to be the optimum level. The optimum working fluid level may also depend on geometry. The heat sink thermal resistance also depends on the heat transfer rate. The resistance initially decreases with the heat transfer rate due to the increase of the boiling heat transfer coefficient. It reaches a minimum and then increases continuously due to dry-out.

The boiling heat transfer presents the largest thermal resistance of the heat sink, above 97% for the prototype tested. The proposed model predicts the data fairly well for the optimum filling ratio provided there is no dry-out. A theoretical analysis shows that, in optimum conditions, the boiling resistance inside the prototype is only slightly smaller than the resistance associated to pure conduction of the conventional heat sink with the same mass and volume. The advantage of the hollow fin vapor chamber heat sink is due to the larger external heat transfer surface area when compared to the conventional heat sink. For the prototype tested, the obtained overall thermal resistance is approximately 20% smaller than in the conventional heat sink. This is because the film resistance represents 70% of the overall thermal resistance of the heat sink.

When compared with a conventional heat sink with the same mass and identical external geometry, the hollow fin vapor chamber prototype presented larger overall sink thermal resistances. However, the conventional heat sink present 4.5 times more mass, which could present economical and dynamic problems.

Further work is needed to enhance the boiling heat transfer inside the heat sink in order to make it competitive to the conventional heat sink. The fine wire screens wick structure seems not to be adequate. Thin layers of sintered copper powder have been reported to be adequate in the literature.

The thermal characterization made here was not made on an optimized heat sink. The prototype parts were made from more easily available stock tubes and sheets, while the manufacturing process employed is not adequate for scale production. The conventional heat sinks employed here are not optimized either. Based on a better understanding of boiling, which is the dominant heat transfer mode inside the vapor chamber, an optimization study similar to the ones encountered in the literature could be employed to assess the advantages of the hollow fin vapor chamber heat sink under a specific application.

References

Molz, M., Mantelli, M. B. H., Milanez, F.H. and Landa, H.G., 2004, "Transient Modeling of a Closed Two-Phase Thermosyphon for Heat Exchanger Applications", 13th International Heat Pipe Conference, Shanghai.

Milanez, F.H. and Mantelli, M.B.H., 2006a, "Thermal characteristics of a thermosyphon heated enclosure", *International Journal of Thermal Sciences*, Vol. 45, pp. 504-510.

Milanez, F.H. and Mantelli, M.B.H., 2006b, "A Loop Thermosyphon for Asphalt Tank Heating", International Heat Pipe Symposium, 2006, Kumamoto.

Angelo, W., Milanez F.H. and Mantelli, M.B.H., 2007, "Design of a Heater for Natural Gas Stations Assisted by Two-Phase Loop Thermosyphon", 14th International Heat Pipe Conference, Florianopolis.

Carey, V.P., 1995, "Liquid-Vapor Phase Change Phenomena", Taylor & Francis, Washington.

Culham, J.R., Khan, W., Yovanovich, M.M., 2001, "The Influence of Material Properties and Spreading Resistance in the Thermal Design of Plate Fin Heat Sinks", paper number NHTC2001-20019, Proceedings of the ASME 35th National Heat Transfer Conference.

Groll, M. and Rosler, S., 1992, "Operation Principles and Performance of Heat Pipes and Closed Two-Phase Thermosyphons", *Journal of Non-equilibrium Thermodynamics*, 17, pp. 91-151.

Incropera, F.P. e de Witt, D.P., 1992, "Fundamentos de Transferência de Calor e de Massa", 3ª. Edição, Guanabara Koogan, Rio de Janeiro, pp. 65-68.

Kaminaga, F., Hashimoto, H., Goto, K. and Matsumura, K., 1997, "Heat Transfer Characteristics of Evaporation and Condensation in a Two-Phase Closed Thermosyphon", Proceedings of the International Heat Pipe Conference Stuttgart, pp. 1-6.

Khan, W., Culham, J.R., Yovanovich, M.M., 2003, "The Role of Fin Geometry in Heat Sink Performance", paper number IPACK2003-35014, Proceedings of the International Electronic Packaging Technical Conference and Exhibition, Maui, Hawaii.

Koito, Y., Motomatsu, K., Imura, H., Mochizuki M. and Saito Y., 2003, "Fundamental Investigations on Heat Transfer Characteristics of Heat Sinks with a Vapor Chamber", Proceedings of the 7th International Heat Pipe Symposium, Jeju, Korea, pp. 247-251.

Mochizuki, M., Mashiko, K., Saito, Y., Nguyen, T., Wu, X. P., Nguyen, T. and Wuttijumnong, V., 2008, "Thermal Management in High Performance Computers by Use of Heat Pipes and Vapor Chambers", Keynote Lecture, Proceedings of the 9th International Heat Pipe Symposium, Malaysia, pp. 39-48.

Mochizuki, M., Nguyen, T., Saito, Y., Horiuchi, Y., Mashiko, K., Sataphan, T. and Kawahara, Y., 2006, "Latest Vapor Chamber Technology for Computer", Proceedings of the 8th International Heat Pipe Symposium, Kumamoto, Japan, pp. 349-353.

Muzychka, Y.S., Culham, J.R., Yovanovich, M.M., 2003, "Thermal Spreading Resistance of Eccentric Heat Sources on Rectangular Flux Channels", *Journal of Electronic Packaging*, 125, pp. 178-185.